2 Center Bifurcation for a Two-Dimensional Piecewise Linear Map

Iryna Sushko and Laura Gardini

2.1 Introduction

It is already well known that the main bifurcation scenario which can be realized considering a business cycle model in dynamic context, is related to a fixed point losing stability with a pair of complex-conjugate eigenvalues. In the case in which such a model is discrete and defined by some smooth nonlinear functions, the Neimark-Sacker bifurcation theorem can be used, described in the previous chapter. While for piecewise linear, or piecewise smooth, functions which are also quite often used for business cycle modeling, the bifurcation theory is much less developed. The purpose of this chapter is to describe a so-called *center bifurcation* occurring in a family of two-dimensional piecewise linear maps whose dynamic properties are, to our knowledge, not well known. Namely, we shall see that in some similarity to the Neimark-Sacker bifurcation occurring for smooth maps, for piecewise linear maps the bifurcation of stability loss of a fixed point with a pair of complex-conjugate eigenvalues on the unit circle can also result in the appearance of a closed invariant attracting curve homeomorphic to a circle. However, differently from what occurs in the smooth case, the closed invariant curve is not a smooth, but a piecewise linear set, appearing not in a neighborhood of the fixed point, as it may be very far from it. In fact, we shall see that the position of the closed invariant curve depends on the distance of the fixed point from the boundary of the region in which the linear map is defined (i.e., from what we shall call critical line LC_{-1}).

We shall describe the global dynamics of a piecewise linear map at the moment of the center bifurcation and after it, comparing the cases in which the map is invertible and noninvertible. For this study we consider a family

of two-dimensional piecewise linear maps $F : \mathbb{R}^2 \to \mathbb{R}^2$ given by

$$F : (x,y) \mapsto \begin{cases} F_1(x,y), (x,y) \in R_1; \\ F_2(x,y), (x,y) \in R_2; \end{cases} \tag{1}$$

where

$$\begin{aligned} F_1 &: \begin{pmatrix} x \\ y \end{pmatrix} \mapsto \begin{pmatrix} (c+a)x - ay \\ x \end{pmatrix}, \\ R_1 &= \{(x,y) : y \le x + d/a\}; \end{aligned}$$

$$\begin{aligned} F_2 &: \begin{pmatrix} x \\ y \end{pmatrix} \mapsto \begin{pmatrix} cx - d + b(x + d/a - y) \\ x \end{pmatrix}, \\ R_2 &= \{(x,y) : y > x + d/a\}. \end{aligned}$$

For convenience, as it will be explained below, we shall assume that the real parameters a, b, c and d satisfy the following conditions:

$$a > 0,\ -(c+1)/2 < b < 1,\ 0 < c < 1,\ d > 0. \tag{2}$$

Our choice of the map F is due to the fact that for $b = 0$ it is a piecewise linear Hicksian multiplier-accelerator model with a lower constraint d, called 'floor', introduced in Chapter 3 and described also in Chapter 6 (the case in which an upper constraint, called 'ceiling', is not involved in asymptotic dynamics). As we shall see, in such a case we have a particular kind of noninvertibility in which a whole half-plane R_2 is mapped into one straight line, so that the map is of so-called $(Z_0 - Z_\infty - Z_1)$ type. While for $b \neq 0$ the map F can be either invertible (for $b > 0$), or noninvertible (for $b < 0$) of $(Z_0 - Z_2)$ type, so that we can compare the results of the center bifurcation in these cases.

The map F is given by two linear maps F_1 and F_2 defined, respectively, below and above the straight line

$$LC_{-1} = \{(x,y) : y = x + d/a\}.$$

The image of this line by F is called *critical line LC or* LC_0:

$$LC_0 = F(LC_{-1}) = \{(x,y) : y = (x+d)/c\},$$

and its image $LC_i = F^i(LC_0)$, $i = 1, ...,$ which is a curve made up by a finite number of linear segments, is also called *critical line (*of higher rank).

Although this notation is more properly used when the map is noninvertible, we keep it in any case. As stated above, invertibility is controlled by the parameter b. For $b > 0$ a point on the right of LC has a unique rank-1 preimage by F_1^{-1} (giving a point in R_1), while a point on the left of LC has a unique rank-1 preimage by F_2^{-1} (giving a point in R_2). Instead, for $b < 0$ a point on the left of LC has no rank-1 preimage, while a point on the right of LC has two distinct rank-1 preimages: One preimage by F_1^{-1} (giving a point in R_1), and the other by F_2^{-1} (giving a point in R_2).

The map F has a unique fixed point $(x^*, y^*) = (0, 0)$ which is the fixed point of the map F_1, while the fixed point of the map F_2 belongs to the main diagonal of the phase plane, which is in R_1, so that it is not a fixed point of F. Using eigenvalues $\lambda_{1,2}$ of the Jacobian matrix of the map F_1, given by

$$\lambda_{1,2} = (a + c \pm \sqrt{(a + c)^2 - 4a})/2, \tag{3}$$

we get that for the parameter range given in (2) the fixed point (x^*, y^*) is attracting for $a < 1$ and repelling for $a > 1$, being a node for $(c + a)^2 > 4a$ and a focus for $(c + a)^2 < 4a$.

Thus, in the range (2) the fixed point loses stability at $a = 1$ with a pair of complex-conjugate eigenvalues crossing the unit circle, so that a *center bifurcation* occurs, which is the main interest of the present chapter. It is clear that in a piecewise linear map the local bifurcation of a fixed point depends only on a corresponding linear map (here F_1), while the global behavior in the phase space depends on the interaction between the other linear maps (which may give rise to any kind of dynamics). In our case, in the region R_2 the map F_2 is defined, so that although the map F has no fixed points in that region, the eigenvalues of F_2, say $\mu_{1,2}$, are important in the global behavior of F. We have

$$\mu_{1,2} = (b + c \pm \sqrt{(b + c)^2 - 4b})/2,$$

so that for $0 < c < 1$ the fixed point of the linear map F_2 is:

- a repelling node for $(c + b)^2 > 4b$ and $b > 1$;
- an attracting node for $(c + b)^2 > 4b$ and $-(c + 1)/2 < b < 1$;
- a flip saddle for $b < -(c + 1)/2$;
- a focus for $(c + b)^2 < 4b$, attracting for $0 < b < 1$ and repelling for $b > 1$.

Here we are interested in the study of the dynamics after the center bifurcation of (x^*, y^*), when the fixed point is an unstable focus and the dynamics are bounded. To this purpose we restrict our analysis to the range of b for which the fixed point of the map F_2 is stable, that is $-(c+1)/2 < b < 1$. Indeed, when the fixed point of the map F_2 is unstable we may have divergent trajectories: If, for example, $b > 1$, then for $a > 1$ (when the fixed point of F is unstable), we have only divergent dynamics, because the two linear maps are both expanding, so that any combination of the two maps is also expanding and no stable cycle can exist. Also for $b < -(c+1)/2$, when the fixed point of the map F_2 is a flip saddle (i.e., with one negative eigenvalue), we may have both bounded and unbounded trajectories. This explains our choice of the parameter range given in (2).

It is clear that when the fixed point (x^*, y^*) of F is stable then it is *globally stable* (because for the range (2) the two linear maps are both contracting, so that any combination of the two maps is also contracting and a repelling cycle cannot exist). While when the fixed point (x^*, y^*) of F is unstable ($a > 1$) we can have bounded dynamics only as long as it is a focus, i.e. for $(c+a)^2 < 4a$ (because when it is a repelling node then all the trajectories are divergent, except for the fixed point).

As remarked above, at $a = 1$ the fixed point (x^*, y^*) undergoes the center bifurcaiton, and the dynamic behavior occurring at this particular bifurcation value is described in the next section. We shall see that independently on the sign of b (invertible or non invertible map) and independently on the type of eigenvalues of the linear map F_2, the map F admits an invariant region, whose size depends on the distance of the fixed point from the critical lines. We shall also comment the global behavior of F (i.e. the dynamics of points outside the invariant region). Then, in the next sections, we shall describe the global behavior of F after the center bifurcation, showing that only the boundary of the region remains invariant, being an attracting closed curve $\mathcal{C}$, and the dynamics of F on $\mathcal{C}$ are either periodic, or quasiperiodic, depending on parameters.

2.2 Dynamics at the Bifurcation Value ($a = 1$)

In this section we first describe the phase portrait of the map F exactly at the bifurcation value $a = 1$. In such a case the fixed point (x^*, y^*) is locally a center: The map F_1 is defined by a rotation matrix (whose determinant equals 1), and it is characterized by a rotation number which may be rational, say m/n, or irrational, say ρ. It is clear that locally, in some neighborhood the fixed point, the behavior of F is that of the linear map F_1, thus we have

a region filled with invariant ellipses, each point of which is either periodic of period n (in case of a rational rotation number m/n) or quasiperiodic (in case of an irrational rotation number ρ). Now the problem we are faced on is to answer the following questions: How big is this region? What is its boundary? What occurs to points outside it? We answer distinguishing the two different cases on the kind of rotation number (rational or irrational).

The invariant region we are looking for clearly is completely included in the region R_1 (i.e., the region of definition for F_1), and it is given by the set of points of R_1 whose trajectories entirely belong to R_1. Thus it must include all the ellipses (invariant for F_1) which are completely included in R_1, so that such a region must necessarily include a region bounded by an invariant ellipse which is tangent to the straight line LC_{-1}. So we can immediately answer to some of the previous questions in the case of an irrational rotation number.

If F_1 is defined by a rotation matrix with an irrational rotation number ρ, which holds for $a = 1$, and

$$c = c_\rho \stackrel{def}{=} 2\cos(2\pi\rho) - 1, \tag{4}$$

then any point from some neighborhood of the fixed point is quasiperiodic, and all the points of the same quasiperiodic orbit are dense on the invariant ellipse to which they belong. (Note that for $c > 0$ we have $\rho < 1/6$). In such a case an invariant region Q exists in the phase space, bounded by an invariant ellipse $\mathcal{E}$ of the map F_1, tangent to LC_{-1}, and, thus, also tangent to LC_i, $i = 0, 1, \ldots$. We can state the following

Proposition 1. *Let $a = 1$, $c = c_\rho$ given in (4). Then in the phase space of the map F there exists an invariant region Q, bounded by an invariant ellipse $\mathcal{E}$ of the map F_1 tangent to LC_{-1}. Any initial point $(x_0, y_0) \in Q$ belongs to a quasiperiodic orbit dense in the corresponding invariant ellipse of F_1.*

Fig.1 shows the invariant region Q of the map F at $a = 1$, $c = 0.4$, $d = 10$. (Indeed, because of numerical precision, we cannot show a true quasiperiodic case, but only its approximation by a periodic case of some high period).

It is clear that such a region also exists (i.e., the region Q defined above) and is invariant, when the map F_1 is defined by a rotation matrix with a rational rotation number, but in such a case Q is not the largest invariant area. In fact, there are also other points outside the tangent ellipse $\mathcal{E}$ which

are periodic with an orbit completely included in the region R_1. For the sake of clarity we shall show this via an example.
So let F_1 be defined by a rotation matrix with a rational rotation number, which holds for $a = 1$, and

$$c = c_{m/n} \stackrel{def}{=} 2\cos(2\pi m/n) - 1, \tag{5}$$

obtained from $\mathrm{Re}\,\lambda_{1,2} = \cos(2\pi m/n)$, then any point in some neighborhood of the fixed point is periodic with rotation number m/n and all the points of the same periodic orbit are located on an invariant ellipse[1].

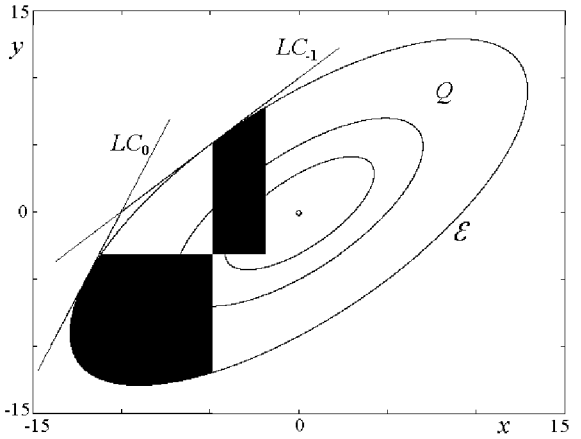

Figure 1: *The invariant region Q of the map F at $a = 1$, $c = 0.4$, $d = 10$. F_1 is associated with an irrational rotation number.*

For short we call *m/n-cycle* a periodic orbit of period n with the rotation number m/n. We can construct the invariant region, say P, existing for $a = 1$ in the phase space by using as an example the case $m/n = 2/13$ (see Fig.2). As noticed above, the region P must include all the invariant ellipses of the map F_1 which are entirely located in the region R_1. That is, P includes a region bounded by an invariant ellipse, say $\mathcal{E}_1$, tangent to LC_{-1}. However there are other periodic orbits belonging to R_1 : Note that there exists a segment $S_1 \subset LC_{-1}$, which we call *generating segment*, such that its end points belong to the same m/n-cycle $p = \{p_1, ..., p_n\}$ located on an invariant ellipse of F_1 which crosses LC_{-1}, denoted $\mathcal{E}_2$ (note that $\mathcal{E}_2$ is

[1]Note that for $c > 0$ we have $m/n < 1/6$.

not invariant for the map F). In our example $S_1 = [p_1, p_7] \subset LC_{-1}$, and $p = \{p_1, ..., p_{13}\}$ is the corresponding $2/13$-cycle. Obviously, the generating segment S_1 and its images by F_1, that is the segments $S_{i+1} = F_1(S_i)$, $S_{i+1} \subset LC_{i-1} = F_1(LC_{i-2})$, $i = 1, ..., 12$, form an invariant polygon P with 13 edges completely included in the region R_1, inscribed in $\mathcal{E}_2$ and whose boundary is tangent to $\mathcal{E}_1$.

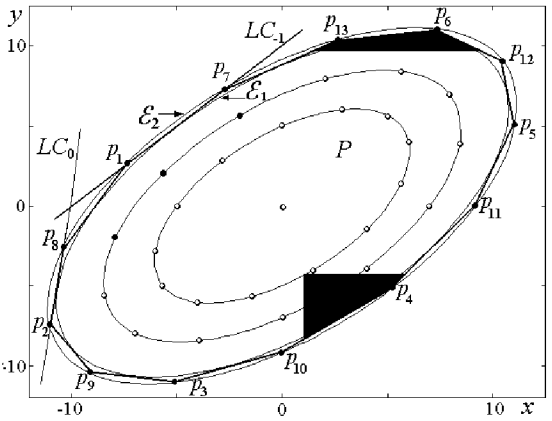

Figure 2: *The invariant polygon P of the map F at $a = 1$, $c = 2\cos(2\pi m/n) - 1$, $d = 10$ and $m/n = 2/13$, so that F_1 is defined by a rotation matrix with the rotation number $2/13$.*

Such a polygon P can be constructed for any rotation number m/n. Summarizing we can state the following

Proposition 2. *Let $a = 1$, $c = c_{m/n}$ given in (5). Then in the phase space of the map F there exists an invariant polygon P with n edges whose boundary is made up by a 'generating segment' $S_1 \subset LC_{-1}$ and its $n - 1$ images $S_{i+1} = F_1(S_i) \subset LC_{i-1}$, $i = 1, ..., n - 1$. Any initial point $(x_0, y_0) \in P$ is periodic with rotation number m/n.*

To end our description of the dynamics at the bifurcation value $a = 1$, we have to clarify the behavior of a trajectory with an initial point (x_0, y_0) which does not belong to the invariant region (either P or Q). It is easy to see that there are the following possibilities:

- If $b = 0$ then the eigenvalues of the Jacobian matrix of F_2 are $\mu_1 = c$, $\mu_2 = 0$, so that any initial point $(x_0, y_0) \in R_2$ is mapped by F_2 in one

step into a point of the straight line LC_0. Then in the case of a rational rotation number it is mapped in a finite number of steps exactly to the boundary of the invariant region P, and ultimately it will be periodic, while in case of an irrational rotation number the generic trajectory tends to the boundary of the invariant region Q.

- For $0 < b < 1$ the fixed point of the map F_2 is an attracting node, the map F is invertible and, thus, the trajectory of any point $(x_0, y_0) \in R_2$ is attracted to the boundary of the invariant region.

- If $-(c+1)/2 < b < 0$ then F_2 is a noninvertible map with an attracting fixed point in R_1. It can be shown that $(x_0, y_0) \in R_2$ is mapped in a finite number of steps to the interior of the invariant region.

We already remarked that in the case $b > 1$ the fixed point of the map F_2 is either a repelling focus (for $(c+b)^2 < 4b$), or a repelling node (for $(c+b)^2 > 4b$), and a trajectory of the map F with initial point (x_0, y_0) not belonging to the invariant region is divergent. While for $b < -(c+1)/2$, the fixed point of F_2 is a flip saddle, and in such a case there may be initial points having divergent trajectories as well as points mapped to the interior of the invariant region. However, as already noticed above, the following consideration is restricted to the range $-(c+1)/2 < b < 1$, so that the fixed point of F_2 is attracting.

The dynamics of the map F at the bifurcation value considered in this section give the name to the *center bifurcation*, and we notice again that the magnitude of the invariant area (P or Q) depends on the distance of the fixed point from the critical line. But we are mainly interested in the description of what occurs 'after', for $a > 1$: We shall see that an invariant region survives after the bifurcation, that is for $a = 1+\varepsilon$ for some sufficiently small $\varepsilon > 0$. However, among all the infinitely many invariant curves existing at the bifurcation only one survives, modified, after the bifurcation: The one which is farthest from the fixed point and gives the boundary of the invariant region. That is, the boundary of the 'old' invariant region is transformed into an attracting closed invariant curve on which the dynamics of F is reduced to a rotation with rational or irrational rotation number.

2.3 Noninvertibility of $(Z_0 - Z_\infty - Z_1)$ Type $(a > 1, b = 0)$

In order to investigate what occurs after the center bifurcation, for $a > 1$, we consider first the map F given in (1) at $b = 0$. It was already mentioned

that in such a case any initial point $(x_0, y_0) \in R_2$ is mapped by F_2 in one step into a point of the critical line LC_0. All consequent iterations by F_2 give points on this straight line approaching the attracting fixed point of F_2 (which belongs to R_1), until the trajectory enters R_1 where the map F_1 is applied. Then the trajectory begins to rotate in the couterclockwise direction, moving away from the unstable focus (x^*, y^*), and in a finite number of iterations it enters the region R_2 where the map F_2 is applied again. Thus, for an orbit the map F_2 plays the role of a return mechanism to the region R_1, and the dynamics are bounded, as longs as the fixed point of F is a focus. Moreover, due to the zero eigenvalue of the map F_2, the dynamics of F are reduced to a one-dimensional subset C of the phase space which is obtained iterating a suitable segment of LC_{-1}. It is easy to see that after a finite number of iterations of LC_{-1} we necessarily get a closed area whose boundary is a closed invariant curve. An example is shown in Fig.3: The closed invariant curve C is obtained by 7 iterations of the segment $[a_0, b_0]$ of $LC_{-1} : C = \cup_{i=1}^{7} F^i([a_0, b_0]))$.

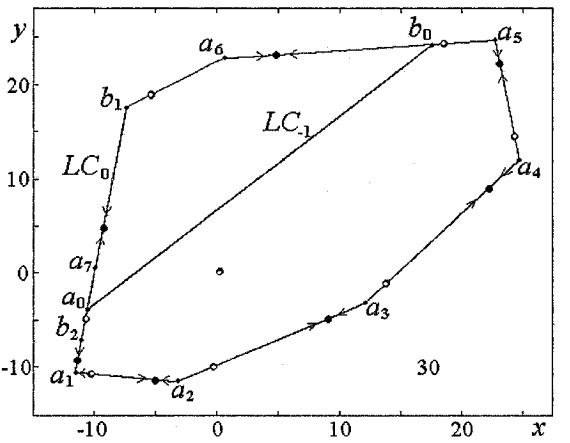

Figure 3: *The attracting closed invariant curve C of the map F at* $a = 1.5$, $b = 0$, $c = 0.15$, $d = 10$. *Points of the attracting and saddle cycles of period 7 are shown by black and white circles, respectively.*

It is clear that any point with initial condition in R_1, except for the fixed point, has a trajectory which spirals away from the fixed point and enters the region R_2 in a finite number of steps, then application of F_2 gives a point

of LC_0, which in a finite number of iterations is mapped into a point of the segment $[a_1, b_1]$ of LC_0. This proves that the closed curve $\mathcal{C}$ is globally attracting for F, except for the fixed point.

We are now interested in the dynamics of F on $\mathcal{C}$. First note that the map F is orientation preserving on $\mathcal{C}$: It can be easily shown that for any three ordered points $u, v, w \in \mathcal{C}$, their images by F are ordered in the same way on $\mathcal{C}$. It follows that we cannot have any folding which means that the restriction of F on $\mathcal{C}$ is invertible and, thus, chaotic dynamics are impossible (indeed, it becomes possible in the case $c < 0$ when there are segments of $\mathcal{C}$ which are folded, but we don't consider this case here). Therefore, we conclude that the dynamics of F on $\mathcal{C}$ are either periodic, or quasiperiodic. If F has an attracting cycle of period n, it has also a saddle cycle of the same period. Fig.3 shows an attracting cycle (node) and a saddle cycle of period 7, and we remark the double meaning of the closed invariant curve: It is the saddle-connection made up of the closure of the unstable set of the saddle (approaching the points of the node), and also the union of a finite number of critical segments. However, in a certain sense the phase portrait of the map F at $a > 1$ is similar to that of a smooth map after the Neimark-Sacker bifurcation: Namely, there exists a closed invariant attracting curve $\mathcal{C}$ on which the map F is reduced to a rotation with rational or irrational rotation number. In contrast to the smooth case, for the map F such a curve is not smooth, but piecewise linear, and it appears not in the neighborhood of the fixed point, but far enough from it: Its location depends on the position of the critical line LC_0.

The considerations given above can be summarized as follows:

Proposition 3. *Let $a > 1, b = 0, (c+a)^2 < 4a$. Then in the phase space of the map F there exists a globally attracting invariant closed curve $\mathcal{C}$ which is a broken line made up by a finite number of images of a segment belonging to LC_{-1}. The dynamics of F on $\mathcal{C}$ are either periodic, or quasiperiodic.*

Fig.4 shows a two-dimensional bifurcation diagram in the (a, c) - parameter plane in which the regions corresponding to different attracting cycles of period $n \leq 32$ are shown by different gray tonalities. If the (a, c) - parameter point belongs to an n-periodicity region, then the map F has an attracting and saddle cycles of period n, located on an attracting closed invariant curve, as stated in proposition 3.

Let us give some comments on the structure of the bifurcation diagram shown in Fig.4. Similar bifurcation diagrams for piecewise linear and piecewise smooth dynamical systems were described in Gallegati *et al.*, 2003,

Hao Bai-Lin, 1998, Sushko *et al.*, 2003, Zhusubaliyev and Mosekilde, 2003. We can note that locally, near the bifurcation line $a = 1$, the periodicity regions look like the Arnol'd tongues described for smooth maps when the Neimark-Sacker bifurcation occurs (although the dynamics are different in the phase space).

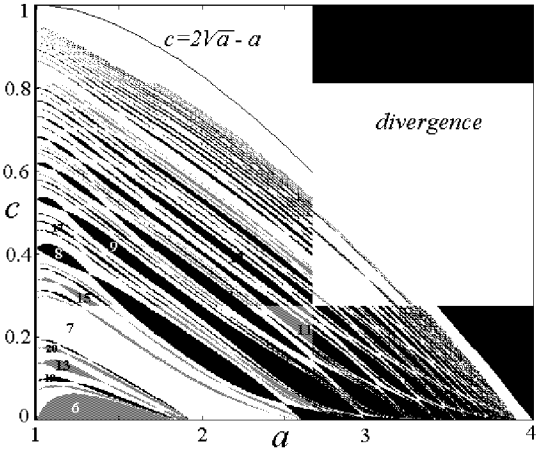

Figure 4: *Two-dimensional bifurcation diagram of the map F in the (a, c)-parameter plane at $b = 0$, $d = 10$. Regions corresponding to attracting cycles of different periods $n \leq 32$ are shown by various gray tonalities.*

It is worth to note that the summation rule which holds for the rotation numbers in the general case with smooth maps, also holds in the piecewise linear case. That is, if m_1/n_1 and m_2/n_2 are two rotation numbers associated with the parameter c_1 and c_2, respectively, at $a = 1$, then also the rotation number $(m_1 + m_2)/(n_1 + n_2)$ exists in between. The white region in Fig.4 is related either to attracting cycles of higher period $n > 32$, or to quasiperiodic trajectories. Indeed, similar to the smooth case, the parameter values corresponding to quasiperiodic trajectories form curves located between the two nearest periodicity regions and issuing from the bifurcation line $a = 1$ at points corresponding to irrational rotation numbers. The so-called 'sausage' structure of the periodicity regions with several subregions is typical for piecewise smooth and piecewise linear systems (see, e.g., Hao Bai-Lin, 1998, Sushko *et al.*, 2003, Zhusubaliyev and Mosekilde, 2003). In fact, different subregions of the same periodicity region of the map F are

related to different compositions of the maps F_1 and F_2 which are applied to get the corresponding cycle (attracting or saddle).

The difference between two-dimensional bifurcation diagrams for a piecewise linear and a smooth map in the case of a center bifurcation or Neimark-Sacker bifurcation, respectively, consists not only in the qualitative shape of the periodicity regions (the 'sausage' structure mentioned above), but also in the kind of bifurcations associated with the boundaries of these regions. It is known that in the smooth case the Arnol'd tongues are bounded by curves corresponding to saddle-node bifurcation and either period-doubling, or Neimark-Sacker bifurcation occurring for the related cycle. While for piecewise linear maps such boundaries are related to *border-collision bifurcations* (see Nusse and Yorke, 1992). In the next section we describe the special case associated with the bifurcation value $a = 1$, while here we describe those associated with the boundaries of the regions for $a > 1$. The border-collision bifurcation, related to the boundary of a periodicity region, involves the merging of the corresponding attracting and saddle cycles, similar to the smooth saddle-node bifurcation, but it is not related to one eigenvalue which become in modulus equal to 1. Instead, it is related to a collision of points of these cycles with the critical line LC_{-1}, i.e. the border separating the regions of different definitions of the map. The waist points of the 'sausage' structure correspond to particular border-collision bifurcations.

The effects of a border-collision bifurcation can be better seen from the dynamics occurring in the phase space (and some times they cannot be understood from a bifurcation diagram). For example, let us add some observations related to the number of the segments of critical lines which form an attracting invariant closed curve $\mathcal{C}$ at $a > 1$, which also may change when a periodic point crosses though LC_{-1}. If we take the (a, c)-parameter point inside the leftmost subregion of a periodicity region shown in Fig.4, related to an attracting m/n-cycle, then the invariant attracting closed curve $\mathcal{C}$ is made up by exactly n segments of the critical lines LC_i, $i = 0, 1, ..., n-1$. It can be shown that in such a case 2 points of the corresponding attracting cycle belong to the region R_2 and $n-2$ points are in R_1. Fig.5 presents an example in the case $m/n = 2/13$, when the curve $\mathcal{C}$ is made up by 13 segments of critical lines. While if the (a, c)-parameter point moves to the next subregions, the number of periodic points in R_2 first increases, and the number of segments of $\mathcal{C}$ decreases (see Fig.6 which shows an example of $\mathcal{C}$ made up by 7 segments in case $m/n = 5/36$), but then, if the (a, c)-point continues to move to the right inside the periodicity region, some periodic points enter R_1 again, so that the numbers of segments of $\mathcal{C}$ increases again.

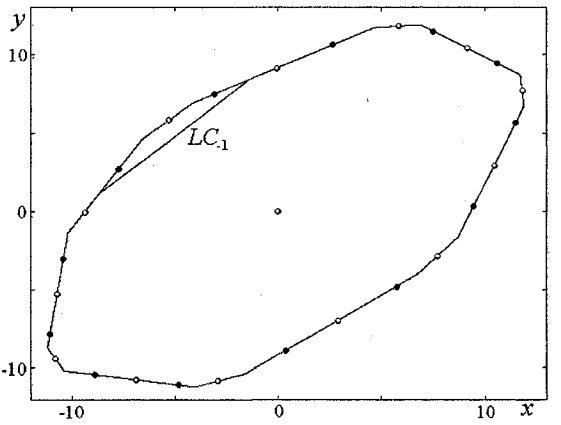

Figure 5: *The attracting closed invariant curve C of the map F made up by* 13 *segments, in the case* $m/n = 2/13$, *at* $a = 1.015$, $c = 0.13613$, $d = 10, b = 0$. *Points of the attracting and saddle cycles are shown by black and white circles, respectively.*

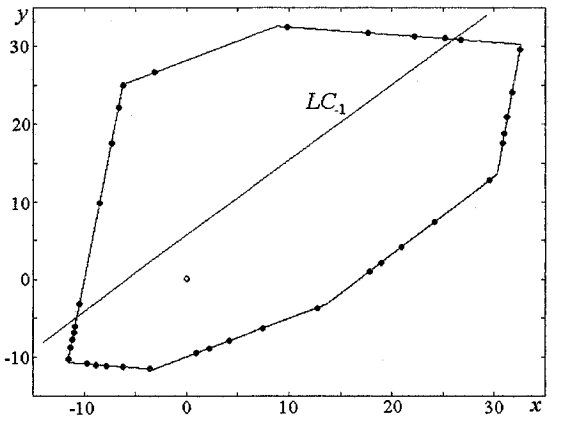

Figure 6: *The attracting closed invariant curve C made up by* 7 *segments, in the case* $m/n = 5/36$, *at* $a = 1.68$, $c = 0.15$, $d = 10$, $b = 0$.

2.4 Border Collision Bifurcations

In the previous section we have presented the bifurcation diagram in the case $b = 0$ (Fig.4) and in the next two sections we shall consider those related with $b \neq 0$. We shall see that when the parameter a belongs to a neighborhood of $a = 1$, i.e., for $a = 1 + \varepsilon$ for some sufficiently small $\varepsilon > 0$, the structure of the periodicity regions is similar for all the range $-(c+1)/2 < b < 1$, and we have a qualitatively similar behavior. That is, the effect of a center bifurcation is the appearance of an attracting closed invariant curve C which is a broken line made up by a finite number of segments when $b = 0$, or by infinitely many segments when $b \neq 0$. Here we describe the effect of the special kind of border collision bifurcation related to a center bifurcation. In Section 2.2 we have described the dynamics at the bifurcation value $a = 1$, which holds for any value of b. Starting from $a = 1$ let us increase a little bit the value of a, entering a periodicity tongue.

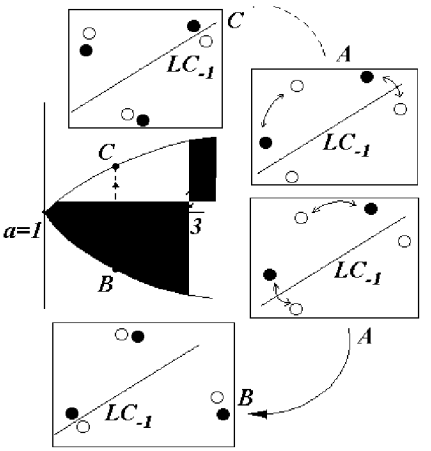

Figure 7: *Qualitative figure of the border-collision bifurcations with few points of the saddles and the attracting nodes shown by white and black circles, respectively.*

To fix the ideas let us consider the case $m/n = 2/13$ used also in Section 2.3. Then the position of the periodic points of the node and the saddle of period 13 at a point $A = (a, c)$ of the tongue shown in Fig.7 is qualitatively the same as the one shown in Fig.5 (also the qualitative shape of the closed

curve C is similar, even if the segments constituting C become infinitely many when $b \neq 0$). Thus, among the infinitely many periodic points existing at the bifurcation value on a segment of LC_{-1}, only two cycles survive, a saddle and a node, having points which are not close to each other. As already remarked in the previous section, only 2 points of the corresponding attracting cycle belong to the region R_2 and $n-2$ points are in R_1, and only 1 point of the corresponding saddle cycle belongs to the region R_2, as it is qualitatively shown in Fig.7 for the parameter point A. Then the effects of the border collisions occurring at the boundaries of the tongue can be easily shown moving the parameter point from A to B and from A to C. As the point A moves towards B, then the points of the saddle cycle moves toward those of the node giving the merging of only one pair of points, as shown in the qualitative picture, which is exactly what occurs in a standard border-collision bifurcation. Thus, periodic points merge and disappear (even if no eigenvalue is equal to 1) when two of them merge on LC_{-1}. A similar behavior, but with the merging of a different pair of periodic points on LC_{-1}, occurs when we move the parameter point from A to C.

2.5 Center Bifurcation for $b > 0$: Invertible Case

In this section we describe the center bifurcation which occurs for the fixed point of the map F given in (1) when the map is invertible, that is for $b > 0$. As already mentioned in the previous sections we assume $a > 1$, $0 < c < 1$ and $(c+a)^2 < 4a$, so that the fixed point of F is an unstable focus. The fixed point of the map F_2, belonging to R_1, is unstable for $b > 1$ (focus for $(c+b)^2 < 4b$ or node for $(c+b)^2 > 4b$) and in these cases all the trajectories of the map F (except for the fixed point) are diverging. Thus, we consider the range $0 < b < 1$.

Let $a = 1+\varepsilon$, $\varepsilon > 0$. The dynamics of F in such a case can be described as follows: A trajectory with an initial point in some neighborhood of the unstable focus (x^*, y^*) rotates under the map F_1 in the couterclockwise direction, moving away from (x^*, y^*), and in a finite number of iterations it necessarily enters the region R_2 where the map F_2 is applied. Then the trajectory under the map F_2 moves back to the region R_1 (given that F_2 has the attracting fixed point in R_1).

For some sufficiently small $\varepsilon > 0$ the dynamics of F are bounded. To see this first note that for b close to 0 the above statement is obvious. For the values of b close to 1, note that at $a = 1$, $b = 1$ we have $F_1 = F_2$, so that if $b \to 1_-$ and $a \to 1_+$ then the distance between the fixed points of F_1 and F_2 tends to 0, so that choosing ε small enough we get a bounded invariant

region. In other words, we can say that the invariant region (Q or P, as described in propositions 1 and 2), existing in the phase space for $a = 1$, exists also after the center bifurcation, but now an inner point of this region, being no longer periodic or quasiperiodic, is attracted from the boundary, as well as an initial point outside the invariant region. Note that due to the invertibility of F a trajectory cannot jump from inside the invariant region to outside and vice versa. For a sufficiently small ε the boundary is an attracting closed invariant curve C, to which the dynamics of F are reduced. It can be shown that for the parameter range considered, the restriction of F to C is invertible, so, as in the previous case ($b = 0$), the trajectory on C is regular.

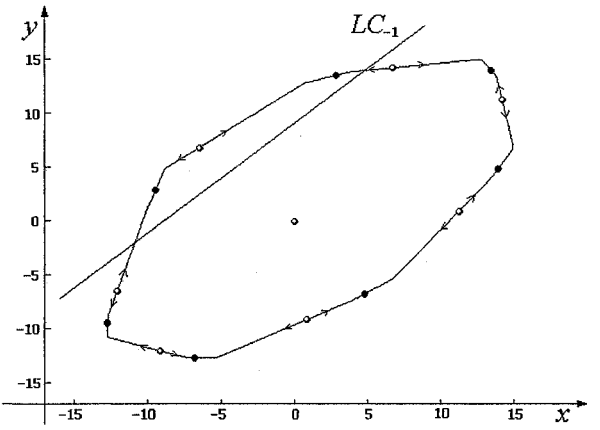

Figure 8: *The attracting closed invariant curve C at $a = 1.1$, $b = 0.1$, $c = 0.25$, $d = 10$. Points of the attracting and saddle cycles of period 7 are shown by black and white circles, respectively.*

Fig.8 presents an example of attracting closed invariant curve C on which the map F is reduced to a rotation with the rotation number $1/7$. That is, there exist an attracting and a saddle cycle of period 7, so that the curve C is formed by the closure of the unstable set of the saddle 7-cycle, approaching the points of the attracting 7-cycle (i.e. a saddle-connection). Differently from the case $b = 0$ in which the curve is made up by a finite number of segments (belonging to the images of LC_{-1}), now it can be shown that there are infinitely many corner points on C, so that it consists of infinitely many linear segments approaching the periodic points of the attracting node.

A typical two-dimensional bifurcation diagram of the map F in the (a, c)-parameter plane for a fixed values of b is shown in Fig.9 where $b = 0.1$. We notice that as long as the fixed point of the map F_2 is an attracting node, that is for $c > c^* = 2\sqrt{b} - b$, which at $b = 0.1$ becomes $c > c^* \approx 0.5325$, the (a, c)-bifurcation diagram looks similar to that of the case $b = 0$ (see Fig.4), and we conjecture that complex dynamics can not occur. While for $c < c^*$ the periodicity regions are stopped on the right by the gray region denoting divergence to infinity, and, as we shall see below, chaotic dynamics may occur, as well as multistability.

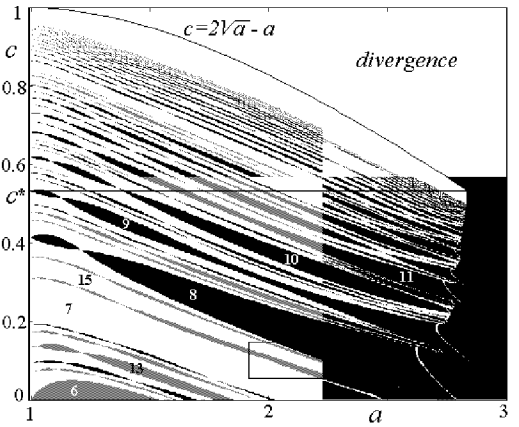

Figure 9: *Two-dimensional bifurcation diagram of the map F in the (a, c)-parameter plane at $b = 0.1$, $d = 10$. Regions corresponding to attracting cycles of different periods $n \leq 32$ are shown by various gray tonalities.*

It is worth to notice that the periodicity tongues shown in the two - dimensional bifurcation diagram correspond to attracting cycles, but they are not necessarily related to closed invariant curves, made up by the saddle-connection. Indeed, we know that for values of a close to 1 the closed invariant curve C exists but increasing a it may be destroyed. Thus let us first give here the possible mechanisms leading to the destruction of a closed invariant curve C which, in a certain sense, are similar to those occurring in the smooth case (to compare, see Aronson *et al.*, 1982):

- A border-collision bifurcation occurring when a point of the attracting cycle and a point of the saddle cycle collide and merge on LC_{-1} and,

as a result, these cycles disappear (Nusse, Yorke, 1992, Banerjee *et al.*, 2000). This bifurcation often occurs on the boundary of a periodicity tongue, as already described in the previous section.

- The attracting n-cycle existing on C may lose stability via flip bifurcation. The result of the flip bifurcation in the piecewise linear case (see Maistrenko *et al.,* 1998) in general is the appearance of a $2n$-cycle of chaotic attractors (i.e., cyclic chaotic attractors made up of $2n$ disjoint pieces), which becomes a one-piece chaotic attractor via a sequence of pairwise merging of the pieces.

- The attracting n-cycle (node) existing on C may become a focus. Indeed, in such a case we can say that a closed invariant curve still exists but is no longer homeomorphic to a circle. Thus this bifurcation denotes a qualitative change of the structure of the invariant curve, but not its disappearance. However, we list it here, as some other authors do, denoting the change of saddle-node connection into saddle-focus one. The saddle-focus connection may be destroyed by a center bifurcation of the n-focus, giving rise to n cyclical closed invariant curves. That is, the closed curve may be destroyed by a center bifurcation occurring in the map F^n.

- The saddle n-cycle may undergo a homoclinic bifurcation. That is, the closed invariant curve is destroyed and replaced by a homoclinic tangle with infinitely many points homoclinic to the saddle (so that also a chaotic repellor exists, made up of infinitely many repelling cycles). As we shall see in the example given below, such a homoclinic tangle may occur inside a periodicity tongue.

In the bifurcation diagram shown in Fig.9 it can also be seen that near the line $a = 1$ the bifurcation structure is similar to the case $b = 0$, but for larger values of a the dynamics become more complicated: As the numerical simulation shows, the periodicity regions can be overlapped, so that the map F can have two coexisting attracting cycles, as well as an attracting cycle coexisting with a chaotic attractor. To give an example, let us enlarge a part of the bifurcation diagram where we have bistability (see Fig.10 with an enlargement of the window indicated in Fig.9, where one of the bistability regions is dashed).

To see which kind of bifurcation occurs when the (a, c)-parameter point crosses the bistability region, let us fix $a = 2.07$, $b = 0.1$ and increase the

value of c (the corresponding parameter path is indicated by the straight line with an arrow in Fig.10). The phase portrait of the map F at $c = 0.07$, and its

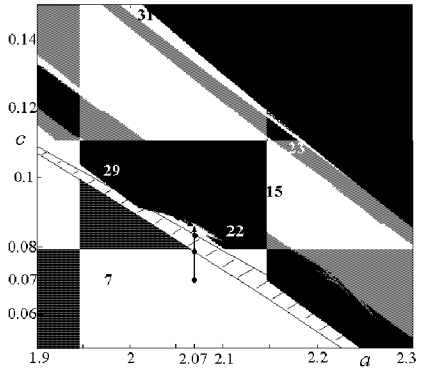

Figure 10: *The enlarged window of Fig.9; A dashed region corresponds to an attracting 7-cycle coexisting with another attractor (regular or chaotic).*

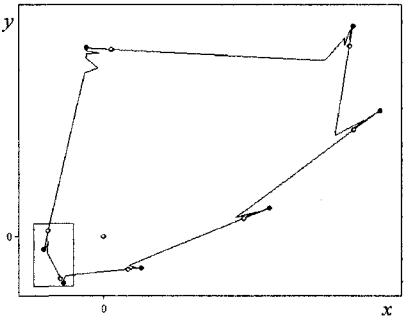

Figure 11: *An attracting closed invariant curve C at $a = 2.07$, $b = 0.1$, $c = 0.07$, $d = 10$. Points of the attracting and saddle cycles of period 7 are shown by black and white circles, respectively.*

enlarged part are shown in Figs.11 and 12(a): An attracting closed invariant curve is formed by the unstable set of the saddle 7-cycle, approaching the points of the attracting 7-cycle, which is the only attractor of the map F.

Fig.12(a) shows also some branches of the unstable set of the saddle, so that it can be seen that stable and unstable sets have no intersection.

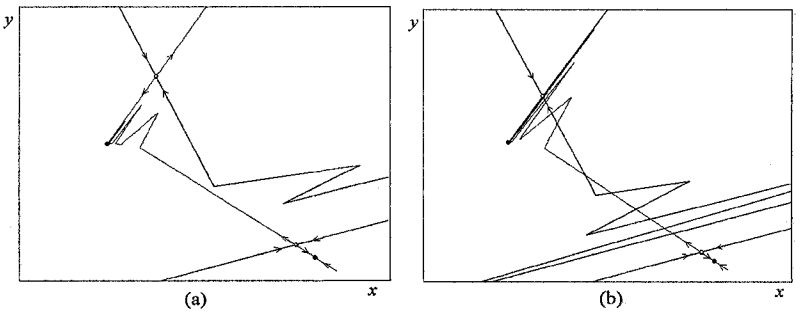

Figure 12: *The enlarged window of the phase portrait of F shown in Fig.11 at $a = 2.07$, $b = 0.1$, $d = 10$ and (a) $c = 0.07$ (before the intersection of the stable and unstable sets of the 7-saddle) (b) $c = 0.074$ in (after the homoclinic bifurcation of the saddle).*

Increasing the value of c, at $c \approx 0.0715$ the first homoclinic bifurcation (or homoclinic contact, the analogue of a homoclinic tangency in smooth maps) occurs for the saddle cycle. After the tangency, the attractor of the map F is still the 7-cycle node, but the closed invariant curve no longer exists: It has been destroyed by the homoclinic tangency and it has been replaced by the homoclinic tangle, with a chaotic repellor. Fig.12(b) presents the enlarged part of the phase space of the map F at $c = 0.074$ during the homoclinic tangle. In order to remark the role of the chaotic repellor and the complex structure of the stable set of the saddle, we show the basins of attraction of the 7 fixed points for the map F^7. For the parameter values used in Fig.12(a), when the unstable set of the saddle gives rise to the closed invariant curve, the stable set of the saddle has a simple structure, and separates the basins (the 7 invariant regions) in a simple way, as shown in Fig.13(a). While for the parameter values used in Fig.12(b), when the unstable set of the saddle intersects the stable one and the closed invariant curve no longer exists, the stable set of the saddle has a complex structure, and separates the basin in a complex way, as shown in Fig.13(b). It is worth to note that the map here is invertible, so that the 7 basins, although with complex structure, must be simply connected (in the next section we shall see instead disconnected basins in the noninvertible case).

On further increasing of the parameter, at $c \approx 0.0777$ the last homoclinic bifurcation (or homoclinic tangency) occurs for the saddle 7-cycle (the related phase portrait is shown in Fig.14(a)). This value of c approximately corre-

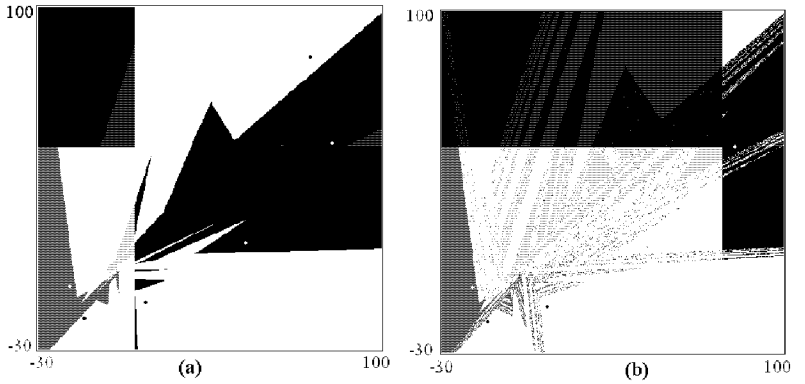

Figure 13: *Baisns of attraction of the* 7 *fixed points of the map* F^7 *(i.e. the 7-cycle of F) at* $a = 2.07$, $b = 0.1$, $d = 10$ *and* $c = 0.07$ *in (a);* $c = 0.074$ *in (b).*

sponds to the crossing of the lower boundary of the bistability region, so that after this bifurcation the map F has the attracting 7-cycle coexisting with a chaotic attractor: Fig.14(b) presents an enlarged part of the phase portrait of F at $c = 0.0778$, where the basins of two attractors are shown by different gray tonalities. The whole phase portrait is shown in Fig.15(a). Note that after the last homoclinic tangency the unstable set of the saddle is not related to a closed invariant curve: One branch tends to the 7-cycle and the other branch tends to the chaotic attractor. While the stable set of the 7-saddle gives the boundary of the two basins of attraction.If we continue to increase the value of c then at $c \approx 0.082595$ a 'saddle-node' border-collision bifurcation occurs when the attracting cycle and the saddle merge and disappear (see Fig.15(b)). This value of c is related to the crossing the upper boundary of the bistability region, so that after the bifurcation the chaotic attractor is the unique attractor of F. We can get the same attractor as a result of a sequence of other bifurcations if the (a, c)-parameter point moves starting from a point inside the 29-periodicity region, for example, $a = 2.025$, $c = 0.0925$. These values corresponds to the attracting and saddle 29-cycles of the map F. If, for example, the parameters change as shown by the thick line with an arrow

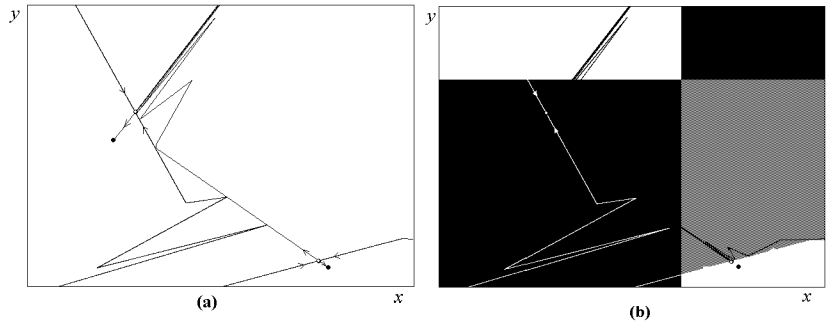

Figure 14: *The enlarged part of the phase portrait of the map* F *at* $a = 2.07$, $b = 0.1$, $d = 10$, *and (a)* $c = 0.0777$ *(near the last homoclinic bifurcation of the saddle 7-cycle); (b)* $c = 0.0778$ *(after the homoclinic bifurcation; The basins of the coexisting attracting 7-cycle and chaotic attractor are shown in different gray tonalities).*

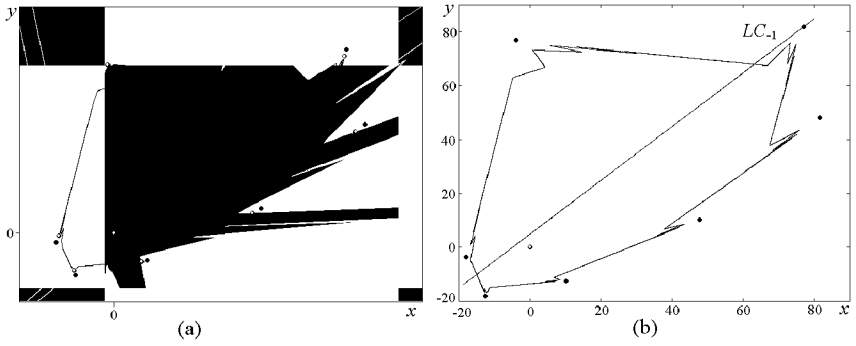

Figure 15: *In (a) phase portrait of the map* F *at* $a = 2.07$, $b = 0.1$, $c = 0.0778$, $d = 10$ *with basins of attraction of coexisting attracting 7-cycle and chaotic attractor. In (b) two attractors of the map* F *at* $a = 2.07$, $b = 0.1$, $c = 0.082595$, $d = 10$, *near the 'saddle-node' border-collision bifurcation when the attracting and saddle 7-cycles merge and disappear due to the collision with* LC_{-1}.

in Fig.10, then at $a \approx 2.05$, $c \approx 0.0872$, the attracting 29-cycle undergoes a flip bifurcation (i.e. the invariant closed curve is destroyed via a flip bifurcation) resulting in a 2×29-cyclic chaotic attractor. Then, after the pairwise merging of the cyclical pieces of the chaotic attractor, the map F has a 29-cyclic chaotic attractor (for example, at $a = 2.056$, $c = 0.0859$), which after further merging of pieces becomes a one-piece chaotic attractor, an example is shown in Fig.15(b).

2.6 Center Bifurcation for $b < 0$: Noninvertible Case

In this last section we describe the center bifurcation occurring in the map F given in (1) when it is noninvertible, for $-(c+1)/2 < b < 0$. We recall that we assume $a > 1$, $0 < c < 1$ and $(c+a)^2 < 4a$, so that the fixed point of F is an unstable focus, while in the given range for b the fixed point of the map F_2, belonging to R_1, is a stable node (with one positive and one negative eigenvalue).

For values of the parameter a in a right neighborhood of 1 the dynamics are qualitatively similar to those occurring in the invertible case, as already remarked in section 2.2 of this chapter. Let us only emphasize the main difference, due to the fact that no point of the phase plane can be mapped in the so called region Z_0, above the critical line LC (as those points are without preimages). For the parameter values taken inside a periodicity tongue the map F still has a pair of cycles, a saddle and a node, and the unstable set of the saddle gives rise to a saddle-node connection, which is a closed invariant curve C made up by infinitely many linear pieces (with corner points). But the area bounded by such a closed curve *is not invariant.* This is due to the fact that arcs which cross the critical curve LC_{-1} are *folded* on the critical line LC creating corner points, whose forward images give again corner points. An example is shown in Fig.16, for parameter values inside a periodicity tongue with rotation number $1/7$. In that figure, the arrows indicate the points of intersection between the invariant curve C and LC_{-1} and two more arrows indicate their images on LC. The non invariance of the area bounded by C is immediately clear from that figure: All the points between the line LC_{-1} and the invariant curve C are mapped outside the area bounded by the curve, between the curve and the critical line LC. That points from outside can be mapped inside the area bounded by C is immediately evident: All the points on the right of LC, belonging to Z_2, have two distinct rank-1 preimages, one on the right and one on the left of LC_{-1}.

Another important difference between the invertible and noninvertible case is related with the unstable set of the saddle cycles: Self intersection

may occur, while it is impossible in invertible maps. This is one more mechanism which causes the destruction of the closed invariant curve C which for noninvertible maps is to be added to the list already given in the previous section. Summarizing in short we can list such mechanisms as follows:

- border-collision bifurcation (which may occur at the boundary of a periodicity tongue);
- flip bifurcation of the attracting cycle on C;
- transition of the node existing on C into a focus (followed by a center bifurcation);
- the saddle may undergo a homoclinic bifurcation (transverse intersections between stable and unstable sets of the saddle);
- the unstable set of the saddle may develop selfintersections, giving infinitely many loops on the invariant curve.

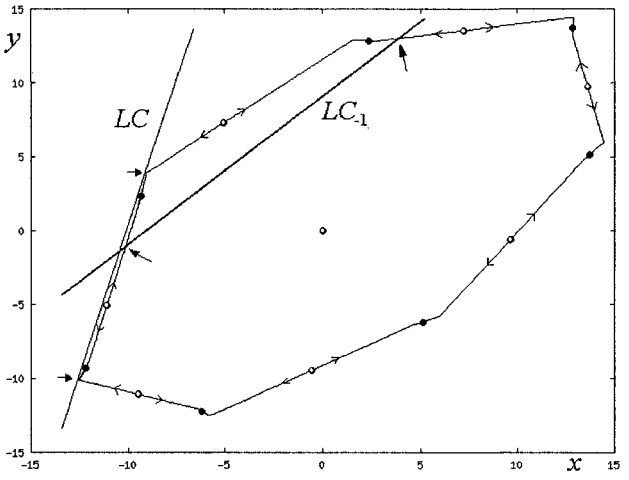

Figure 16: *The attracting closed invariant curve C at* $a = 1.1$, $b = -0.05$, $c = 0.25$, $d = 10$.

Let us illustrate the last kinds of bifurcations by an example, taking the parameter values in the periodicity tongue associated with the rotation number $1/6$, shown in the bottom-left of the (a, c) parameter plane of Fig.17.

Let us fix $a = 1.1$, $b = -0.4$ and increase the value of c (the corresponding parameter path is indicated by the straight line with an arrow in Fig.17).

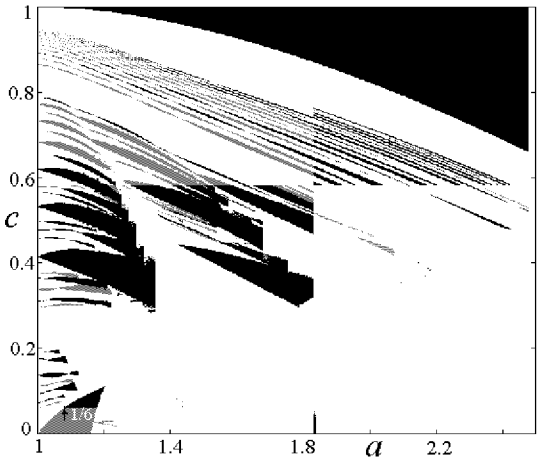

Figure 17: *Bifurcation diagram in the* (a, c) *parameter plane at* $b = -0.4$ *and* $d = 10$.

The phase portrait of the map F at $c = 0.05$ has a unique attractor: a stable node of period 6, and in Fig.18 (a) we present the basins of attraction of the 6 fixed points for the map F^6 (black points in the figure). The stable set of the saddle cycle (white points in the figure) gives the basin boundary. While the unstable set of the saddle is an invariant set which is no longer homeomorphic to a circle, as self intersections already exist. This is shown by an enlarged part of the phase space in Fig.18 (b).

In Fig.18 (a) one more peculiarity of noninvertible maps can be seen: The basins are not simply connected. However the disjoint portion of the basin shown there is entirely included in the region Z_0 so that it has no other preimages. While increasing the value of c, at $c = 0.06$ that portion of the basin intersects the critical curve LC thus giving a portion in the region Z_2 and this small portion has infinitely many preimages, clearly visible in Fig.19 (a). The related unstable set of the saddle is still with self intersections, as shown in the enlargement of the phase space in Fig.19 (b), but is it also possible to see that it is now close to the stable set of the same saddle (basin boundary in Fig.19 (a)), and this denotes that a homoclinic bifurcation is going to occur.

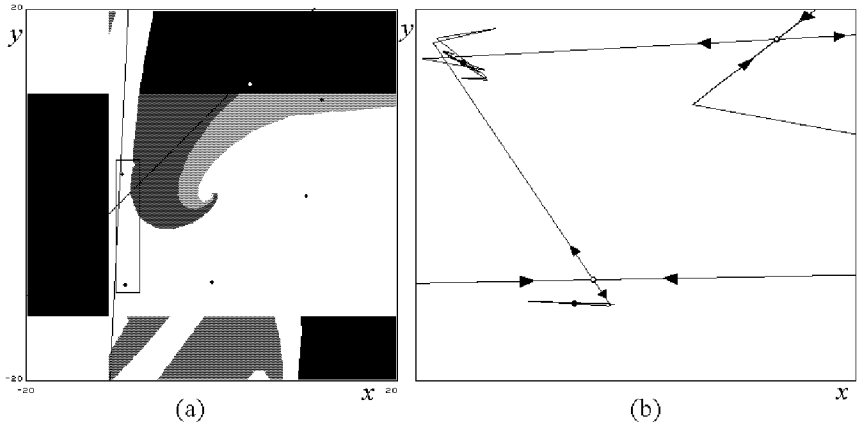

Figure 18: *(a) Basins of attraction of the* 6 *fixed points of the map* F^6 *at* $a = 1.1$, $b = -0.4$, $c = 0.05$*; (b) The enlarged part of (a) with some branches of the stable and unstable sets of the saddle* 6*-cycle.*

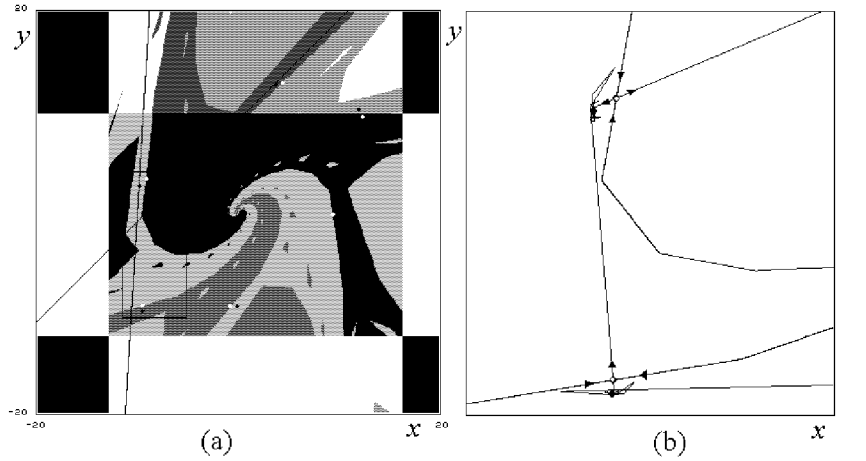

Figure 19: *(a) Basins of attraction of the* 6 *fixed points of the map* F^6 *at* $a = 1.1$, $b = -0.4$, $c = 0.06$*; (b) The enlarged part of (a) with some branches of the stable and unstable sets of the saddle* 6*-cycle, near a homoclinic bifurcation.*

In fact, Fig.20 (a) ($c = 0.0615$) shows the homoclinic tangency and Fig.20 (b) ($c = 0.064$) shows the homoclinic transverse intersections between the stable and unstable sets. It is clear that a strange repellor also exists in such a regime, with the homoclinic tangle of the saddle cycle, and this can be seen in the complex structure of the basins, with many disconnected component in a fractal structure, as shown in Fig.21.

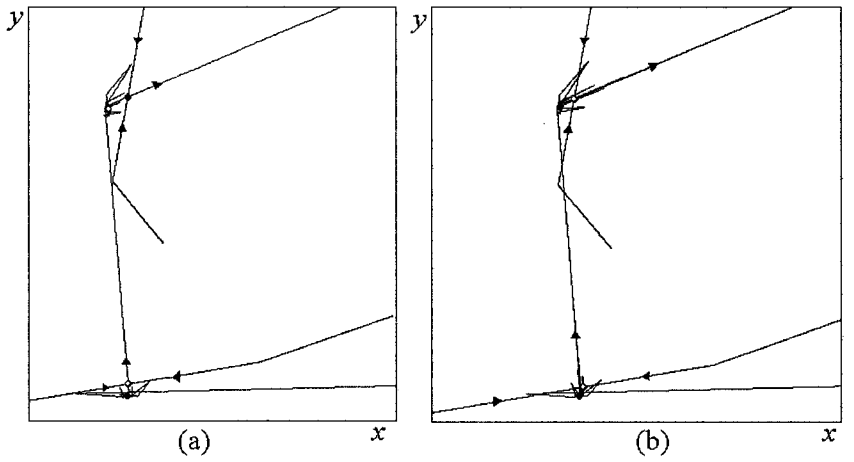

Figure 20: *The enlarged part of the phase space with some branches of the stable and unstable sets of the saddle* 6*-cycle at* $a = 1.1$, $b = -0.4$, $c = 0.0615$ *(a) and* $c = 0.064$ *(b).*

It is worth noticing one more property of the noninvertible maps, which is the existence of absorbing areas inside which all the asymptotic dynamics occur. Consider for example the case shown at $c = 0.064$, for which a strange repellor exists: We can say that all the unstable cycles constituting the strange repellor must belong to the annular absorbing area shown in Fig.22 (a). This area can easily be constructed by taking the images of the critical curves. In fact, an invariant area has necessarily the boundary given by the images of the segment of LC_{-1} belonging to the area itself, which is called *generating segment*[2] (see, e.g., Mira *et. al.*, 1996). In our case, by taking 6 images of that segment we get the external boundary of a simply

[2]Given a noninvertible map F and an invariant area A (i.e., such that $F(A) = A$), the generating arc is defined by $A \cap LC_{-1}$.

connected invariant area, which includes also the unstable fixed point. But as it is an unstable focus, we can also construct an annular absorbing area by taking more images of the same segment. In fact, with 6 more iterations we get the inner boundary of an area of annular shape shown in Fig.22 (a). It is clear that any point of the phase space belonging the hole around the unstable focus is such that its trajectory enters the annular area and never escapes. This means that all the limit set of the trajectories belongs to that annular area, in particular all the cycles of F, except for the focus fixed point.

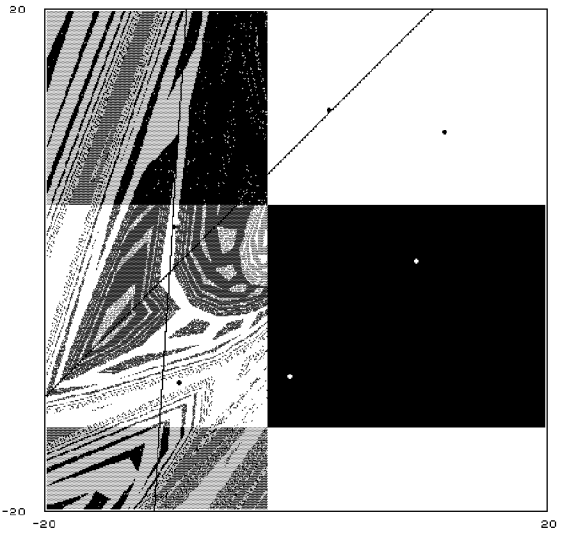

Figure 21: *Basins of attraction of the* 6 *fixed points of the map* F^6 *at* $a = 1.1$, $b = -0.4$, $c = 0.064$.

As it can be seen from Fig.21, the points of the stable node (black points) and those of the saddle (white points) are very close to each other, and on further increase of c the parameter point reaches the boundary of the periodicity tongue, where a saddle-node merging occurs via a border-collision bifurcation. After such bifurcation the pair of 6-cycles disappear and the map F is left with a chaotic attractor: That is, the chaotic repellor existing in the annular area shown in Fig.22 (b), is transformed into a chaotic attractor with knots and self intersection.

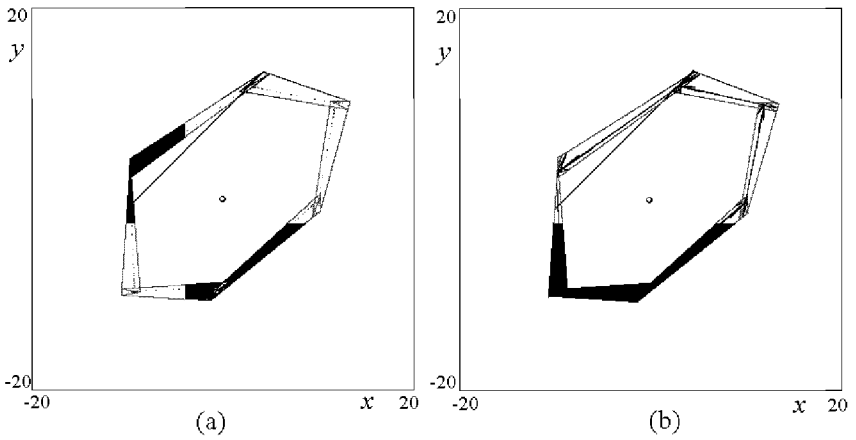

Figure 22: *The annular absorbing area of the map F at* $a = 1.1$, $b = -0.4$, $c = 0.064$ *(a) and* $c = 0.071$ *(b).*

References

Afraimovich, V.S., Shil'nikov, L.P., 1983, "Invariant two-dimensional tori, their destruction and stochasticity", *Gorkii University*, Gorkii, Russia, pp. 3-26.

Aronson, D.G., Chory, M.A., Hall, G.R., McGehee, R.P., 1982, "Bifurcations from an invariant circle for two-parameter families of maps of the plane: A computer-assisted study", *Commun. Math. Phys.* 83, pp. 303-354.

Banerjee, S., Ranjan, P., Grebogi, C., 2000, "Bifurcations in Two-Dimensional Piecewise Smooth Maps - Theory and Applications in Switching Circuits", *IEEE Trans. Circuits Syst.-I: Fund. Theory Appl.* 47 No. 5, pp. 633-643.

Boyland, P.L., 1986, "Bifurcations of circle maps: Arnol'd tongues, bistability and rotation intervals", *Commun. Math. Phys.*, 106, pp. 353-381.

Guckenheimer, J., Holmes, P., 1983, *Nonlinear Oscillations, Dynamical Systems, and Bifurcations of Vector Fields.* Springer-Verlag.

Gumovski, I., Mira. C., 1980, *Recurrences and Discrete Dynamical Systems*. Springer-Verlag.

Hao Bai-Lin, 1989, *Elementary Symbolic Dynamics and Chaos in Dissipative Systems*. World Scientific, Singapore.

Hommes, C.H., 1991, *Chaotic dynamics in economic models.* Wolters-Noodhoff, Groningen.

Hommes, C.H., Nusse, H., 1991, "Period three to period two bifurcations for piecewise linear models", *Journal of Economics* 54(2), pp. 157-169.

Kuznetsov, Y., 1995, *Elements of applied bifurcation theory.* Springer-Verlag.

Maistrenko, Y., Sushko, I., Gardini, L., 1998, "About two mechanisms of reunion of chaotic attractors", *Chaos, Solitons & Fractals*, 9(8), pp. 1373-1390.

Mira, C., Gardini, L., Barugola, A., Cathala, J.C., 1996, *Chaotic dynamics in two-dimensional noninvertible maps.* Singapore, World Scientific.

Nusse, H.E., Yorke, J.A., 1992, "Border-collision bifurcations including "period two to period three" for piecewise smooth systems", *Physica D*, 57, pp. 39-57.

Sushko, I., Puu, T., Gardini, L., 2003, "The Hicksian floor-roof model for two regions linked by interregional trade", *Chaos Solitons & Fractals*, 18, pp. 593-612.

Zhusubaliyev, Z.T., Mosekilde, E., 2003, *Bifurcations and Chaos in Piecewise-Smooth Dynamical Systems*, Singapore, World Scientific.